

Thin film deposition with time varying temperature

T. A. de Assis

Instituto de Física, Universidade Federal da Bahia, Campus Universitário da
Federação, Rua Barão de Jeremoabo s/n, 40170-115, Salvador, BA, Brazil

E-mail: thiagoaa@ufba.br

F. D. A. Aarão Reis

Instituto de Física, Universidade Federal Fluminense, Avenida Litorânea s/n,
24210-340 Niterói RJ, Brazil

E-mail: reis@if.uff.br

Abstract. We study the effects of time-dependent substrate/film temperature in the deposition of a mesoscopically thick film using a statistical model that accounts for diffusion of adatoms without lateral neighbors whose coefficients depend on an activation energy and temperature. Dynamic scaling with fixed temperature is extended to predict conditions in which the temperature variation significantly affects surface roughness scaling. It agrees with computer simulation results for deposition of up to 10^4 atomic layers and maximal temperature changes of $30K$, near or below the room temperature. If the temperature decreases during the growth, the global roughness may have a rapid growth, with effective exponents larger than $1/2$ due to the time-decreasing adatom mobility. The local roughness in small box size shows typical evidence of anomalous scaling, with anomaly exponents depending on the particular form of temperature decrease. If the temperature increases during the growth, a non-monotonic evolution of the global roughness may be observed, which is explained by the competition of kinetic roughening and the smoothing effect of increasing diffusion lengths. The extension of the theoretical approach to film deposition with other activation energy barriers shows that similar conditions on temperature variation may lead to the same morphological features. Equivalent results may also be observed by controlling the deposition flux.

PACS numbers: 68.55.-a, 68.35.Ct, 81.15.Aa , 05.40.-a

1. Introduction

The morphological properties of a growing film by vapor techniques are mainly determined by the balance between substrate/film temperature and pressure. High temperature helps the system to attain equilibrium states, for instance favoring formation of smooth surfaces in homoepitaxy, while the increase of pressure leads to faster adsorption and drives the system far from the equilibrium conditions [1]. For these reasons, many statistical models of thin film growth represent the competition of the external flux of atoms or molecules and temperature-dependent surface processes, such as diffusion, aggregation, and reactions [2, 3, 4].

The main quantity to characterize surface morphology is the roughness, which measures thickness fluctuations along the film surface. It may be measured for the whole surface (global roughness) or inside a box that slides on that surface (local roughness). The scaling properties with time and size are described by dynamic relations [3], which are called normal when local and global fluctuations scale with the same exponents [5] and anomalous when local and global exponents are different [6, 7, 8, 9, 10].

A question of experimental relevance is the effect of changing physico-chemical conditions during film growth. For example, a recent experimental work on electrodeposition of Prussian Blue films interpreted the growth as a process dominated by surface diffusion in which the time-increasing adsorption rate is responsible for an anomaly in the dynamic scaling relation [11]. The problem of spontaneous fluid imbibition in a porous medium is another system that shows anomalous scaling (AS) and is modeled as interface growth with time-dependent couplings [12].

This scenario motivated theoretical works on growth models where the microscopic rules of aggregation change in time. Ref. [13] showed that a sudden change in the parameters of the Edwards-Wilkinson (EW) growth equation [14] may be responsible for nontrivial effects in roughness scaling, such as power-law relaxation to steady states. The AS in stochastic growth equations with time-dependent couplings was discussed in Ref. [15] and illustrated for the EW equation with time-dependent surface tension, showing good agreement with numerical results for models of spontaneous imbibition [16, 17]. In lattice models of film growth, AS was recently shown in competitive models with time-varying probabilities [18].

On the other hand, to our knowledge no work have already discussed the effects of time-varying temperature in thin film deposition. For this reason, this paper is devoted to study a model of deposition and diffusion of adsorbed species in which the diffusion coefficients are affected by a time-dependent substrate/film temperature. For simplicity, the model assumes that only adatoms in terraces can move, while atoms with lateral neighbors are permanently aggregated. A combination of a theoretical approach and simulation results shows several nontrivial effects on surface roughness scaling that may help to understand experimental results. In cases of decreasing temperature, there is evidence of AS for film thicknesses typical of real mesoscopically thick films. Moreover, the global roughness has a nontrivial evolution which does not allow a reliable calculation of a growth exponent. In cases of increasing temperature, a non-monotonic evolution of the global roughness may be observed, possibly with a saturation for a wide range of film thickness. The main advance from previous works is to show those features in feasible conditions of film growth, since the model is an approximate description of low-temperature physical vapor deposition. Possible extensions to deposition models with several activation energy barriers suggest that

the same features may be observed in similar conditions.

The rest of this paper is organized as follows. In Sec. 2, we will define the model, review basic concepts of dynamic scaling of surface roughness, and discuss properties of the model for fixed temperature. In Sec. 3, a theoretical approach for time-dependent temperature is developed to predict conditions in which the roughness scaling is affected or not. In Sec. 4, we will discuss results for some conditions of decreasing temperature. In Sec. 5, we will discuss results for some conditions of increasing temperature. In Sec. 6, the extension of our approach to other models is discussed. In Sec. 7, we summarize our results and present our conclusions.

2. Basic definitions and concepts

2.1. Model definition and simulations

The model studied in this work was introduced in Ref. [19]. It is a solid-on-solid type model (no overhang in the film surface) and the deposit has a simple cubic lattice structure. The substrate is flat, at the xy plane, with linear size L ($L \times L$ columns), with the lattice parameter being the length unit. The column height is the z coordinate of the topmost adatom. There is an external flux of F atoms per site per unit time, measured in number of monolayers (ML) per second. An incident atom is adsorbed upon landing above a previously deposited atom or a substrate site. All adsorbed atoms with no lateral and no upper neighbor diffuse with coefficient D (number of steps per unit time). If an adatom has a lateral or an upper neighbor, then it is permanently aggregated at that position. Fig. 1 illustrates the possible steps of some mobile atoms at the film surface.

The diffusion coefficient D depends on temperature as

$$D = \nu_0 \exp(-E/k_B T), \quad (1)$$

where ν_0 is a jump frequency and E is the activation energy in a flat surface, which typically amounts to tenths of eV. The parameter

$$R \equiv D/F \quad (2)$$

quantitatively represents the interplay between temperature and pressure and determines the film properties. The other relevant parameter is the film thickness t , proportional to the deposition time.

In the submonolayer growth regime, this model corresponds to irreversible island growth with critical nucleus of size $i = 1$, which was already applied to several systems [4]. The irreversible lateral aggregation is a reasonable assumption for low temperature or large atomic flux, although it does not respect detailed balance conditions. This model also has the advantage of reducing simulation times compared with models where all atoms are mobile. The aggregation condition is similar to the Das Sarma and Tamborenea (DT) model of molecular beam epitaxy [20], but the main difference is that the DT model and its extensions restrict the adatom diffusion to finite distances. Moreover, the model does not consider Ehrlich-Schwebel (ES) barriers for downhill movement at terrace edges [21] and does not allow uphill movement because adatoms with lateral neighbors are immobile. Indeed, our aim is to consider a model with a minimal set of relevant parameters, in order to search for features that are intrinsically related to the time-varying temperature.

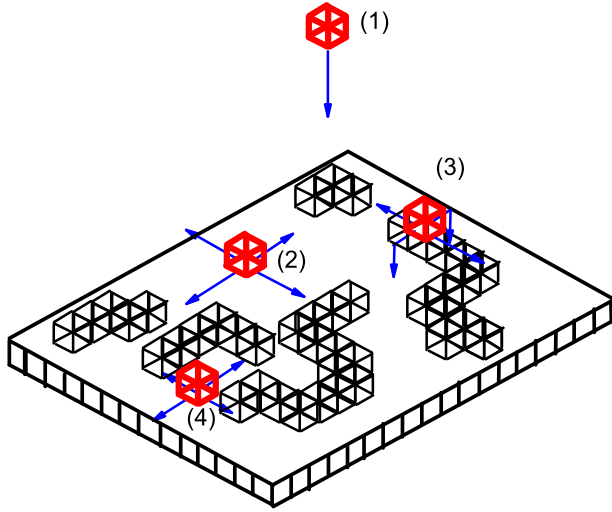


Figure 1. Illustration of the model: deposition of an atom (1); adatom diffusion in terraces (2), with possibility of downhill movement and irreversible aggregation (3), and with possibility of irreversible aggregation at a step edge (4).

Simulation results presented here were obtained in lattices with $L = 512$. Some results were also obtained in $L = 256$ and $L = 1024$ in order to confirm that finite-size effects are negligible in the simulated time range. Fixed deposition parameters are $\nu_0/F = 10^{14}$ and the activation energy $E = 0.6\text{eV}$. These values are reasonable compared to experimental data for several metals and semiconductors, although the direct applicability is limited due to the differences in lattice structure and aggregation assumptions [22, 4]. Choosing a fixed value of E and changing T does not restrict our conclusions because the physically important parameter is R , which is a function of E/T . In all cases, the temperature is uniform across the film and may vary in time. Some results for fixed temperature are also obtained for comparison.

We will consider temperature values in which R ranges between 10^1 and 10^5 . These values are small if compared to works on submonolayer growth, which frequently consider R up to 10^9 [4]. However, they are suitable for low temperature deposition, which is a necessary condition for the applicability of a model with irreversible attachment to steps (in other words, even with a small binding energy to a lateral neighbor, the relative probability of an attached atom to move will be small). For $R = 10^5$, results of Ref. [19] show that adatoms execute an average of 28 random steps before aggregation, thus diffusion lengths in terraces are much smaller than the lateral size of the films and finite-size effects are negligible.

During the growth of a sample, the adsorption of each new atom takes place in a time interval $1/(FL^2)$. After this process, R/L^2 steps of randomly chosen free atoms are performed. Since R/L^2 is usually not integer, and it may be small for large L , we

keep its fractional part for determining the number of steps after the next adsorption events. If the temperature changes during the film growth, then the value of R is updated after the deposition of each complete layer (L^2 atoms), which corresponds to a unit time interval.

2.2. Dynamic scaling of surface roughness

The global roughness (or interface width) is defined as

$$W(L, t) \equiv \left\langle \overline{(h - \bar{h})^2} \right\rangle^{1/2}, \quad (3)$$

where the overbars represent spatial averages and the angular brackets represent configurational averages over various samples. For short deposition times (small thicknesses), effects of the finite substrate size L are negligible and W scales as

$$W \sim t^\beta, \quad (4)$$

where β is called the growth exponent.

For comparison with experimental data, the local roughness $w(r, t)$ is more useful. It is also defined as a root mean square height fluctuation, but the spatial average is limited to a box of size r , with $r < L$, and the configurational average is performed by gliding this box over the film surface and over various samples. In the regime of thin film growth (negligible effects of substrate size), it follows the Family-Vicsek (FV) dynamic scaling relation [5]

$$w(r, t) \approx Ar^{\alpha_l} g\left(\frac{Bt}{r^z}\right). \quad (5)$$

Here, α_l is the local roughness exponent (sometimes called Hurst exponent), z is the dynamic exponent, B is a constant, and g is a scaling function such that $g(x) \sim 1$ for $x \gg 1$ (small box size) and $g(x) \sim x^{-\alpha_l/z}$ for $x \ll 1$ (large box size, where the local roughness coincides with the global one).

In systems with normal scaling, the amplitude A in Eq. (5) is a constant (time-independent), thus $\beta = \alpha_l/z$ and the global roughness exponent α equals the local one. A scaling analysis of $w(r, t)$ of several growth models in one- and two-dimensional substrates is presented in Ref. [23]. In systems with AS, the amplitude A scales as

$$A \sim t^\kappa, \quad (6)$$

with κ characterizing the degree of anomaly [8]. A FV relation can also be defined for the global roughness and involves the exponent α , but it is useful only if very long times / large thicknesses are attained.

2.3. Previous works

Here we restrict the discussion to results on two-dimensional substrates (growth in $2 + 1$ dimensions), which is the subject of the present work.

Several models with diffusion of all adatoms and energy barriers proportional to the number of neighbors were previously studied in fixed temperature. Some authors proposed that they had AS [28] or a logarithmic scaling of amplitude A in the FV relation [29]. Wilby et al [30] showed that the growth exponent β was close to value of the universality class of the fourth order nonlinear growth equation of Villain, Lai

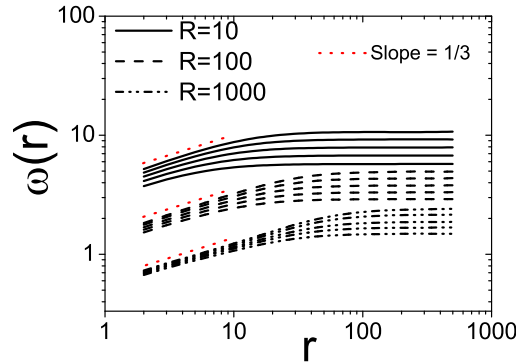


Figure 2. Local roughness as a function of box size for $R=10$ (full line), $R=100$ (dashed line) and $R=1000$ (dashed dotted dotted line) at times $t = 500ML$, $1000ML$, $2000ML$, $4000ML$ and $8000ML$, from bottom to top. The dotted line indicates the slope value of $1/3$.

and Das Sarma (VLDS) [31, 32]. Recent renormalization studies explained the long crossover to VLDS scaling [33, 34].

The model presented in Sec. 2.1 was already studied numerically, showing a FV relation for the global roughness that includes the R -dependence as [19]

$$W = \frac{L^\alpha}{R^x} f(R^y t / L^z), \quad (7)$$

with $\alpha \approx 2/3$, $z \approx 10/3$, $x \approx 0.5$, and $y \approx 1$. The exponents α and z agree with those of the VLDS class [3, 35, 36]. The values of exponents x and y were explained by scaling arguments [19].

For $R \geq 10^5$, the surface roughness of this model is very small, even with very large thicknesses (10^4 or 10^5 ML) [19]. This is not a regime of dynamic scaling, which is an additional reason for our simulations to be performed with smaller values of R . Full diffusion models with values of R of the same order may show larger roughness, particularly if ES barriers are included [37], but with an extended set of parameters.

2.4. Scaling of local roughness in constant temperature

A recent work on numerical integration of the VLDS equation showed evidence of AS in $2 + 1$ dimensions [38], which raises the question on a possible AS in our lattice model. This feature was not investigated in Ref. [19].

We performed simulations of the model with $10 \leq R \leq 1000$ for fixed R (fixed temperature). Fig. 2 shows the local roughness as a function of box size for three values of that parameter. For $R = 10$, there is a split in the curves for small r , which suggests AS. However, that split tends to disappear as the thickness increases. For instance, from $t = 4000ML$ to $t = 8000ML$, the change in the local roughness for $r = 5$ is only 7%. For $R = 100$ and $R = 1000$, the split of the curves is almost negligible for $t > 10^3$. For those reasons, we understand that there is no asymptotic AS in our lattice model with fixed R , and an apparent anomaly appears only for small R and for small thicknesses due to some type of scaling correction.

Fig. 2 also shows that the local roughness scales with $\alpha_l \approx 1/3$ for small r [Eq. (5)]. This exponent is significantly below the VLDS value $\alpha_l = \alpha \approx 2/3$ [36]. This discrepancy is not a failure of theoretical predictions, but a consequence of scaling corrections also observed in other growth models [23].

3. Theoretical approach to temperature varying conditions

In competitive models involving two different aggregation dynamics, a FV relation similar to Eq. (7) is obtained, with the probability p replacing the ratio R and exponents x and y depending on the competing components [24, 25]. When p slowly changes in time, the surface roughness evolution is predicted by substituting the time-dependent form of that parameter in the corresponding FV relation [18]. This is supported by simulation results of several competitive models [18].

Relation (7) in the growth regime (where finite-size effects are negligible) gives

$$W = B \frac{t^\beta}{R^\Delta} \quad , \quad \beta = 0.2 \quad , \quad \Delta = 0.3, \quad (8)$$

where B is a constant and the exponents β and Δ were obtained from the values of α , z , x , and y . The data for constant R gives $B \approx 3.3$ [19].

In order to understand the conditions in which a temperature change has a significant effect in the roughness evolution, we consider the rate of variation of the surface roughness:

$$\frac{dW}{dt} = B \frac{t^{\beta-1}}{R^\Delta} [\beta - \Delta s(t)] \quad , \quad s(t) \equiv \frac{E}{k_B T} \frac{d \ln T}{d \ln t}. \quad (9)$$

The extension of Eq. (8) to time varying R is a reasonable assumption only if the roughness change is of the same order or smaller than that of the fixed temperature case. In these cases, the system responds to the slowly varying conditions with normal kinetic roughening in a short time scale. This is expected for $|s(t)| \lesssim 1$.

When $|s(t)| \ll 1$, the roughness evolves similarly to the constant temperature case. This is the case of small $\frac{E}{k_B T}$ (very high temperatures, in which the surface is always very smooth) and of very slow changes of temperature (when changes in $\ln T$ are much smaller than 1 after growth of several layers).

If $|s(t)| \sim 1$, then the roughness changes are significantly different from the constant temperature case. If $s(t)$ is weakly dependent on time, then the rate of roughness increase is changed by a nearly constant factor and W will scale with the exponent β of constant temperature. On the other hand, if $s(t)$ varies in time, plots of $\log_{10} W \times \log_{10} t$ may show effective growth exponents very different from β . If the temperature increases in time, $s(t)$ is negative and the roughness may decrease in time.

Finally, if $|s(t)| \gg 1$, the growth conditions are rapidly changing and Eq. (9) suggests that it controls the roughness evolution. Under these conditions, it is not expected that the extension of Eq. (8) to time varying R is correct, since the system may not be able to adapt to varying growth conditions with its normal kinetic roughening behavior. Thus, Eq. (9) may not apply. Moreover, the hypothesis of rapidly changing conditions may also rule out the thermal equilibrium hypothesis of Eq. (1) adopted along the whole surface. For this reason, the case $|s(t)| \gg 1$ is not considered here.

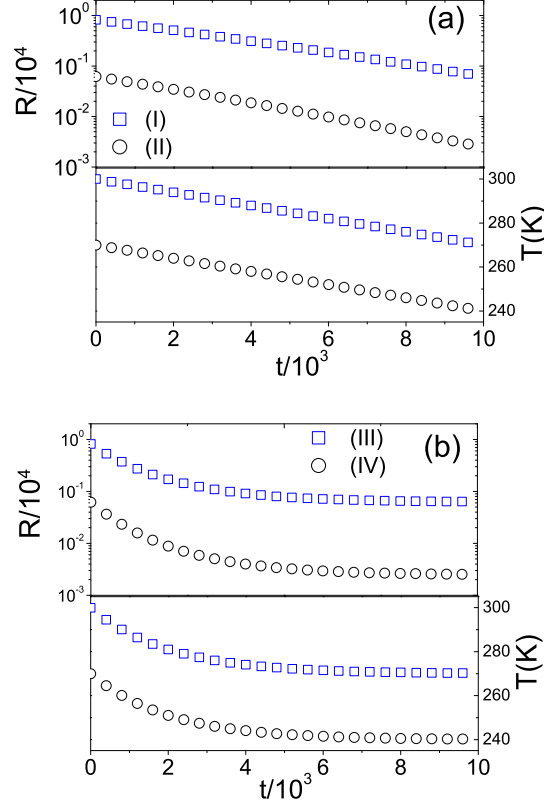


Figure 3. (a) Parameter R as a function of the thickness, considering $E = 0.6\text{eV}$, $\nu_0/F = 10^{14}$, and temperature variation of cases (I) and (II). Squares correspond to case (I) and circles to case (II). (b) Parameter R as a function of the thickness, considering $E = 0.6\text{eV}$, $\nu_0/F = 10^{14}$, and temperature variation of cases (III) and (IV). Squares correspond to case (III) and circles to case (IV).

4. Deposition with decreasing temperature

These are situations with slow down of the diffusion process, thus roughening is facilitated as the deposition evolves.

4.1. Temperature variation

First we consider linearly decreasing temperature during the time interval for deposition of $t_{max} = 10^4 ML$, numbered cases (I) and (II), whose conditions are specified in Table 1. This value of t_{max} is reasonable for mesoscopic films, giving thicknesses of a few micrometers for most materials. Figs. 3a shows the time evolution of the parameter R and of the temperature in those cases.

We also consider cases of exponential convergence of the temperature to the final value, with a characteristic time/thickness $t_c = 2000 ML$, so that:

$$T = T_F + (T_I - T_F) \exp(-t/t_c). \quad (10)$$

Case Number	Temperature Variation	Thickness Dependence	T_I (K)	T_F (K)
I	Decreasing	Linear	300	270
II	Decreasing	Linear	270	240
III	Decreasing	Eq. 10	300	270
IV	Decreasing	Eq. 10	270	240
V	Increasing	Linear	240	270
VI	Increasing	Linear	270	300
VII	Increasing	Eq. 10	240	270
VIII	Increasing	Eq. 10	270	300

Table 1. In all the cases we considered the deposition of $t_{max} = 10^4 ML$.

The conditions of cases (III) and (IV) considered here are presented in Table 1. Deposition of $t_{max} = 10^4 ML = 5t_c$ layers is considered, thus the final temperatures of the films are very close to T_F . These cases represent systems exchanging heat by conduction with a colder reservoir (e. g. an initially heated system separated from the surroundings by a conducting wall).

Fig. 3b shows the corresponding time evolution of the parameter R and temperature. The main difference from the linear decays of cases (I) and (II) is that R rapidly decreases at short times (up to $t \sim t_c$) and slowly decreases during most of the deposition time. When $t \sim t_{max}$, the temperature is approximately constant (T_F).

In cases (I) to (IV), $E = 0.6eV$ in the room temperature range, thus $E/k_B T \sim 23$. Maximal temperature changes are close to 10% of the initial ones, from 1 to 10^4 monolayers, thus $\frac{d \ln T}{d \ln t} \sim 0.01$. This gives $s \sim 0.2$ [Eq. (9)], which is expected to give a significant change in the roughness scaling (Sec. 3). Depending on the particular form that the temperature varies, larger or smaller values of s may be obtained in different time ranges, as shown below.

The control of these temperature changes are realistic for thin film growth. For comparison, in film deposition with the substrate subject to a temperature gradient, much larger temperature differences are established [26, 27]. An example is *FePt* film growth with the temperature varying from $250^\circ C$ to $600^\circ C$ along a substrate distance smaller than $1cm$ [26]).

4.2. Global roughness scaling

Fig. 4a shows the evolution of the global roughness of the films in cases (I) and (II) and the theoretical predictions from Eq. (8) with the time-dependent R shown in Fig. 3a. Those predictions are close to the simulation data when the roughness is larger than 1. The discrepancy for $W \lesssim 1$ is expected because scaling relations are not expected to apply for small roughness. The local slope of the plots in Fig. 4a are effective exponents β_{eff} .

For small thicknesses ($t \leq 10^3 ML$), the slope β_{eff} is close to the VLDS value $\beta \approx 0.2$. This corresponds to one tenth of the total growth time and the temperature change is only $3K$, thus it is a growth with nearly constant temperature. For case (I), the roughness is typically smaller than unity, thus it is not a true scaling region where a reliable estimate of β can be measured. For larger thicknesses ($t \geq 10^3 ML$), W rapidly increases in cases (I) and (II). For $5 \times 10^3 ML \leq t \leq 10^4 ML$, the effective

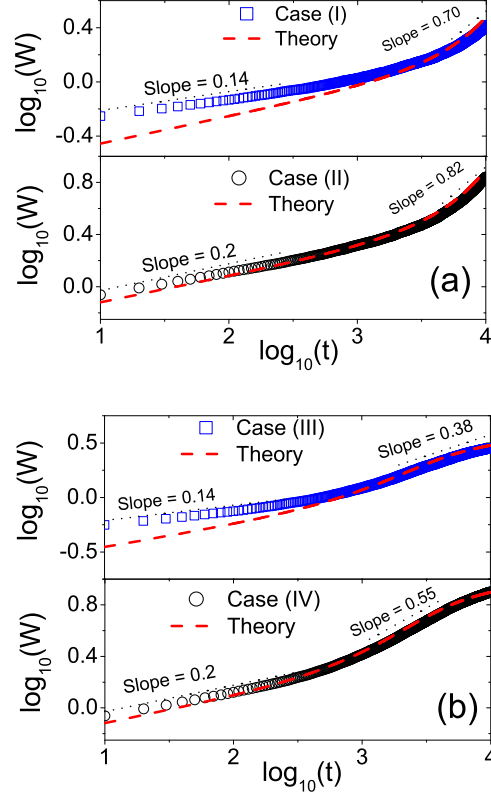


Figure 4. (a) Global roughness as a function of the thickness for cases (I) and (II). Squares correspond to case (I) and circles to case (II). The dashed line indicate the theoretical predictions from Eq. (8) with the time-dependent R shown in Fig. 3a. (b) Global roughness as a function of the thickness for cases (III) and (IV). Squares correspond to case (III) and circles to case (IV). The dashed line indicate the theoretical predictions from Eq. (8) with the time-dependent R shown in Fig. 3b.

exponents are $\beta_{eff} \approx 0.70$ and $\beta_{eff} \approx 0.82$, respectively (see Fig. 4a).

The evolution of the global roughness for cases (III) and (IV) is shown in Fig. 4b and also compared with the extension of Eq. (8) to time-dependent R (Fig. 3b). Again, W increases slowly for small thicknesses, but shows large effective exponents β_{eff} for thicknesses above $10^3 ML$. In case (IV), where R decreases almost two orders of magnitude during the film growth, $\beta_{eff} > 1/2$ is found, similarly to cases (I) and (II). As t approaches t_{max} , the slopes of the plots in Fig. 4b tend to decrease due to the temperature saturation.

The continuously increasing β_{eff} , which attains large values at longer times, represents a nontrivial evolution of the roughness. This is solely a consequence of the time decreasing temperature during deposition, which reduces diffusion lengths and facilitates roughening. The agreement with the theoretical approach of Sec. 3 supports this interpretation.

Some models and experiments show large values of β_{eff} , but for different reasons.

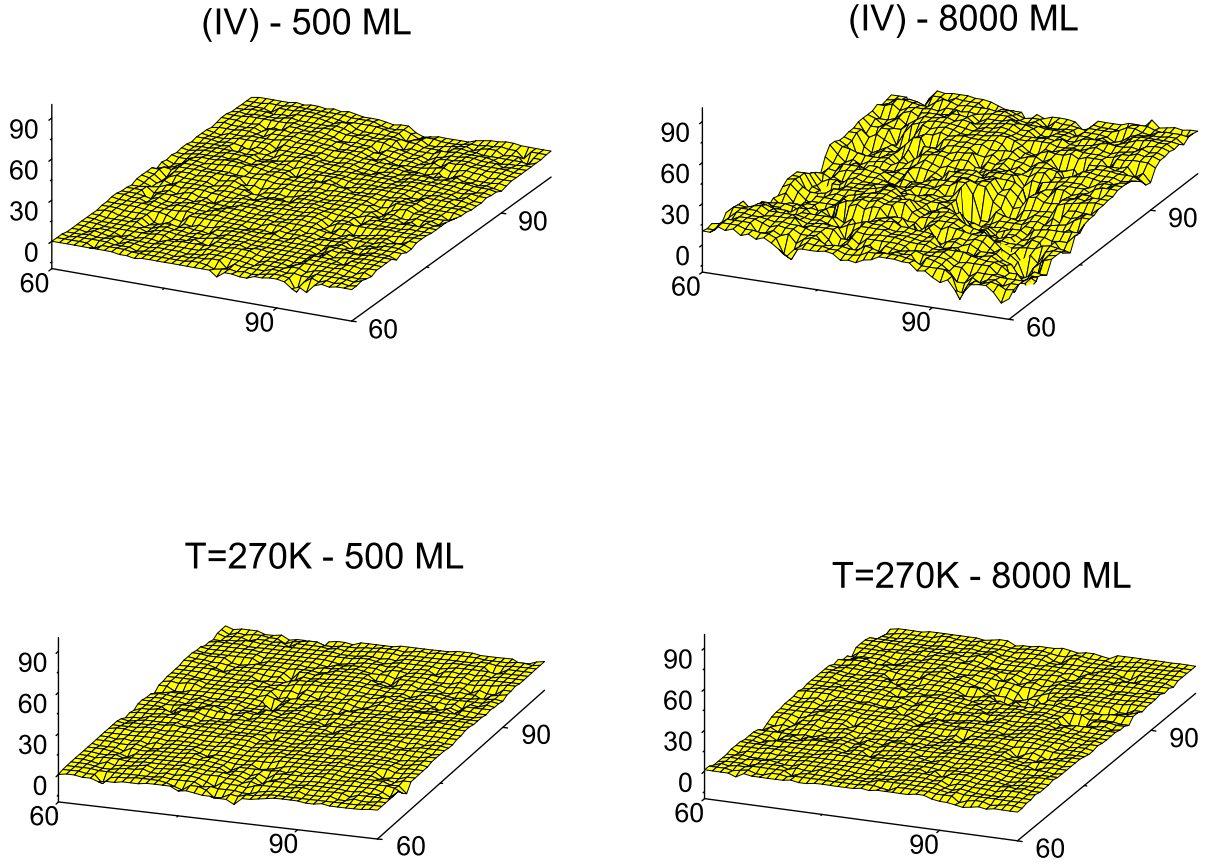


Figure 5. Surface topography of films with thicknesses $t = 500ML$ and $t = 8000ML$ in (top) case (IV) and (bottom) with fixed temperature $T = 270K$.

An example is Ag/Ag(100) growth, where mound steepening leads to a crossover from very smooth surfaces (up to $25ML$) to very rough ones (up to $1000ML$) at $300K$ [39]. In that case, the presence of ES barriers [21] is responsible for the crossover. Some systems also have $\beta > 1/2$ as a consequence of preferential aggregation at surface hills instead of valleys (possibly with surface instability) or shadowing effects [40, 41]. However, in our model, none of those mechanisms are present.

Fig. 5 shows the surface topography of films with thicknesses $t = 500ML$ and $t = 8000ML$ in case (IV) and with fixed temperature $T = 270K$. The film grown in fixed temperature is always smooth, but a remarkable roughening is observed in the film grown with decreasing temperature. In the latter, there is no evidence of mound formation, columnar growth, or any other geometrical feature that frequently explains the large values of β_{eff} . Instead, the nontrivial evolution of the roughness is

a consequence of the decreasing temperature.

We also recall that the scaling in systems with competitive growth dynamics is very different from Figs. 4a-b, since they usually show two scaling regions with $\beta_{eff} \leq 1/2$. Moreover, large β is not necessarily related to large roughness. For instance, very rough deposits are produced by grain deposition models [42] and have $\beta \sim 0.1$, which is much smaller than the value of the asymptotic Kardar-Parisi-Zhang class [43].

For the above reasons, if a nontrivial increase of the roughness is observed in an experimental work, one must consider the possibility that the temperature is changing during the deposition, since this seems to be the simplest mechanism responsible for that feature. Alternatively, the possibility of time-increasing adsorption rates may be considered, as in Ref. [11] (where $\beta \approx 0.5$ was obtained), since they also lead to time-decreasing R .

4.3. Local roughness scaling

The local roughness in cases (I) and (II) is shown in Fig. 6a as a function of the box size r , for several thicknesses in the range $500ML < t < 8000ML$. There is a significant split of the curves for small r , in contrast to the small split shown in Fig. 2 for constant temperature (note that vertical and horizontal scales are the same in Figs. 2 and 6a). This is an AS feature, with the FV relation [Eq. (5)] having time-dependent amplitude A .

Fig. 6b shows the local roughness as a function of box size for cases (III) and (IV), respectively. These plots also show evidence of AS due to the split of the curves for small r . This trend persists for thicknesses $t > 2t_c$, where the temperature is changing very slowly.

The AS, corresponding to the continuous increase of local slopes, is another feature intrinsically related to the slow down of surface diffusion. Indeed, reduced adatom mobility is known to facilitate the formation of steep surface features at small lengthscales.

For small and constant r , the time scaling of the amplitude A [Eqs. (5) and (6)] characterizes the AS. The inset of Fig. 6a shows $w(r = 10, t)$ (proportional to A) as a function of time in cases (I) and (II). It increases faster than the power-law of Eq. (6), particularly for the longest times. On the other hand, the inset of Fig. 6b shows the scaling of $w(r = 10, t)$ for cases (III) and (IV), which approximately follow power laws with anomaly exponents $\kappa = 0.28 \pm 0.01$ (III) and $\kappa = 0.47 \pm 0.02$ (IV). This reinforces the evidence of AS in plausible conditions for experimental work only due to the decreasing temperature.

It is important to stress that the AS found in cases (III) and (IV) is an apparent scaling restricted to the thickness range studied here. At long times, the temperature saturates at T_F , thus the deposit will attain the characteristic features of films grown with fixed temperature. Such films do not have AS, but have normal VLDS scaling (Sec. 2.4). Furthermore, in cases (I) and (II), the temperature decrease is necessarily limited to a finite time range, thus there is no asymptotic scaling. These features contrast with the true AS of the lattice models in Ref. [18], but those models were not so closely related to real film growth.

Finally, we observe that the local roughness exponents measured in Figs. 6a and 6b are close to $1/3$, similarly to the constant temperature case (Sec. 2.4).

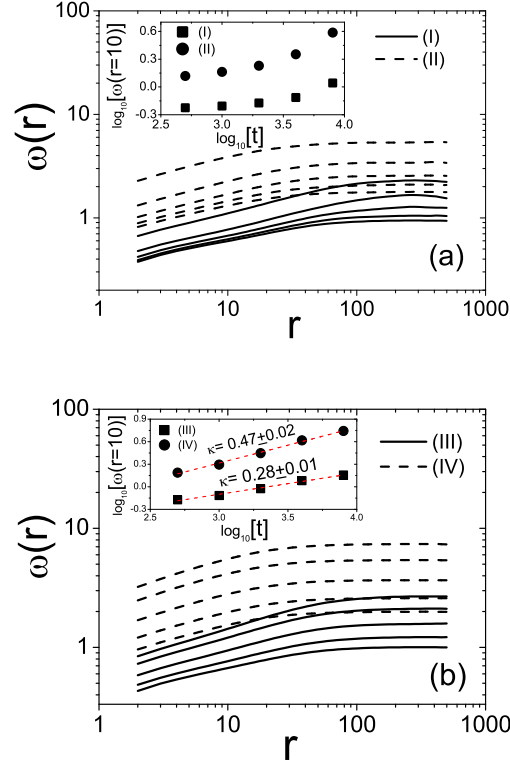


Figure 6. (a) Local roughness as a function of box size for cases (I) (solid lines) and (II) (dashed lines) at times $t = 500ML, 1000ML, 2000ML, 4000ML$ and $8000ML$, from bottom to top. The inset shows $\log_{10}(\omega)$ as a function of $\log_{10}(t)$ for $r = 10$ in cases (I) (squares) and (II) (circles). (b) Local roughness as a function of box size for cases (III) and (IV), respectively, at times $t = 500ML, 1000ML, 2000ML, 4000ML$ and $8000ML$, from bottom to top. The inset shows $\log_{10}(\omega)$ as a function of $\log_{10}(t)$ for $r = 10$ in cases (III) (squares) and (IV) (circles). The dashed lines indicate the linear fits for the κ evaluation. The corresponding values of κ are also shown.

5. Deposition with increasing temperature

We also consider two cases of linearly increasing temperature, numbered (V) and (VI) in Table 1, again from $t = 0$ to $t_{max} = 10^4 ML$. Fig. 7a shows the time evolution of the parameter R and of the temperature. The situation with exponential convergence of temperature [Eq. (10) with $T_I < T_F$] is considered in cases (VII) and (VIII), also described in Table 1, with characteristic decay time $t_c = 2000ML$. Fig. 7b shows the corresponding time evolution of the parameter R and of the temperature.

Fig. 8a shows the evolution of the global roughness in cases (V) and (VI) and the comparison with Eq. (8) extended to time-dependent R case shown in Fig. 7a. Again, deviations from the theoretical prediction are large only when the global roughness is very small ($W \lesssim 1$, i. e. smaller than the lattice parameter).

The nontrivial result in Fig. 8a is the nonmonotonic variation of the roughness.

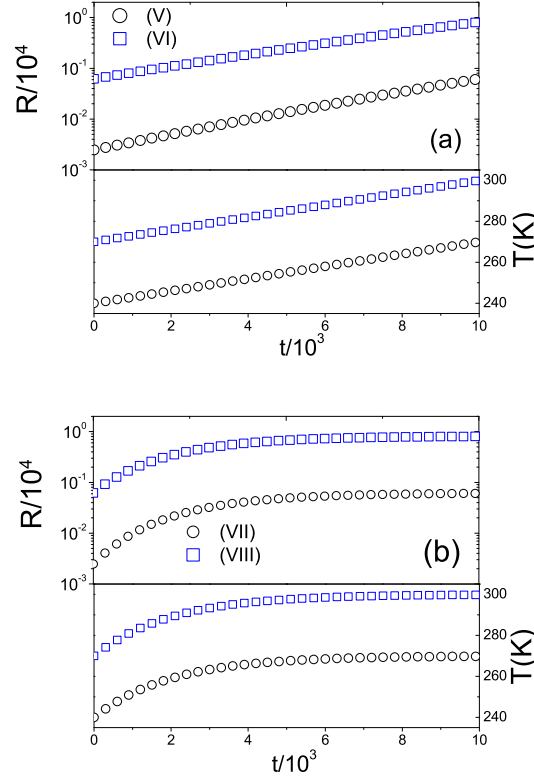


Figure 7. (a) Parameter R as a function of the thickness, considering $E = 0.6\text{eV}$, $\nu_0/F = 10^{14}$, and temperature variation of cases (V) and (VI). Circles correspond to case (V) and squares to case (VI). (b) Parameter R as a function of the thickness, considering $E = 0.6\text{eV}$, $\nu_0/F = 10^{14}$, and temperature variation of cases (VII) and (VIII). Circles correspond to case (VII) and squares to case (VIII)

It increases for short times due to spread of correlations and excitation of modes of increasing wavelength, as usual in kinetic roughening [3, 44]. However, it attains a maximum and begins to decrease due to the smoothing effect of large diffusion coefficients. The effect is more pronounced for smaller temperatures because the relative increase of R is larger.

Fig. 8b shows the evolution of the global roughness in cases (VII) and (VIII), with the comparison with the theoretical prediction for time-dependent R case shown in Fig. 7b. W presents a maximum at small thicknesses in the former and a plateau in the latter. These effects are similar to those of the linearly increasing T [(V) and (VI)]. However, for larger thicknesses, the roughness slowly increases. This is expected because the temperature saturates at $t \sim t_{max}$, thus the usual feature of kinetic roughening (roughness increasing in time) is observed.

The presence of extremal values in the roughness (a maximum and a minimum) was already shown in other models, but not as an effect of changing temperature. For instance, in an electrodeposition model of Ref. [45], the adsorption rate had a maximum, which corresponds to a minimum of an effective diffusion-to-deposition

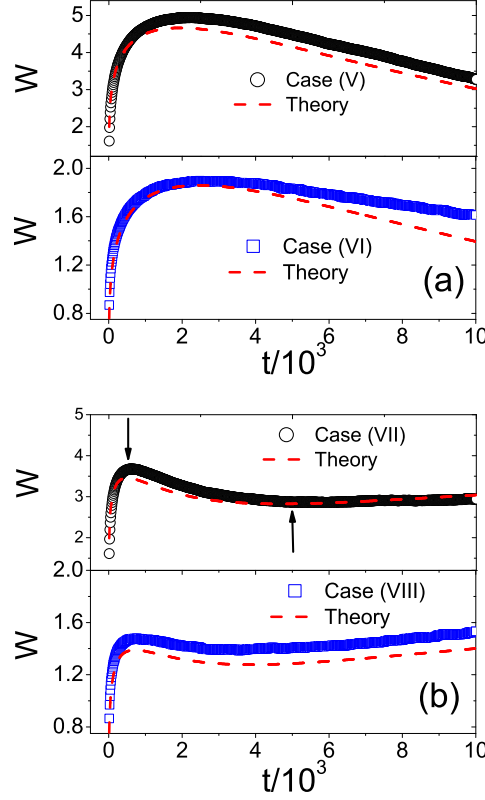


Figure 8. (a) Global roughness as a function of the thickness for cases (V) and (VI). Circles correspond to case (V) and squares to case (VI). The dashed line indicate the theoretical predictions from Eq. (8) with the time-dependent R shown in Fig. 7a. (b) Global roughness as a function of the thickness for cases (VII) and (VIII). The dashed line indicate the theoretical predictions from Eq. (8) with the time-dependent R shown in Fig. 7b. The arrows indicate a maximum and a minimum of global roughness. Circles correspond to case (VII) and squares to case (VIII).

rate R . The increase of R after that minimum seems to be responsible for the effect of reducing the roughness in a certain time window, similarly to our model. Pal and Landau [46, 47] also showed that deposition with large R may lead to roughness oscillations at short times, due to fluctuations between partial and complete filling of the first atomic layers. However, those oscillations disappear after deposition of approximately 10 layers (maybe less), in contrast to our models.

6. Possible extensions of the model

As shown in Secs. 4 and 5, the theoretical predictions of Sec. 3 for time-dependent R fit the simulation data quite well when the roughness is not very small. Thus, that approach may help to predict conditions for observing the same phenomena observed here, such as AS and rapid roughness increase (large β_{eff}) for decreasing temperature

and roughness oscillations for increasing temperature.

In a more complex growth model, other temperature-dependent parameters are relevant, typically in the form of Boltzmann factors involving other activation energies. Let us recall, for instance, the studies of submonolayer island dynamics where all adatoms are mobile. This is the case of the Clarke-Vvedensky model [48], in which activation energies are proportional to the number of lateral neighbors. The additional parameter ϵ is related to the lateral binding energy and the scaling of average island size contains factors in the form $R^a \epsilon^b$, with exponents a and b of order 1, related to the nature of the model and possibly to the lattice structure [49, 50].

In the growth of a thin film, assuming that an additional parameter ϵ is present, the FV relation for short times and constant temperature is expected to give

$$W = C \frac{t^\beta}{R^\delta \epsilon^\gamma}, \quad (11)$$

where β is the exponent of the universality class of the model (possibly not VLDS) and δ and γ are exponents of order 1.

The brackets in the right-hand side of Eq. (9) separate the roughness variation in two terms, the second one related to variable temperature. Using Eq. (11), this time-dependent term is

$$s(t) \equiv \left(\frac{E}{k_B T} - \gamma / \delta \ln \epsilon \right) \frac{d \ln T}{d \ln t}. \quad (12)$$

Again, $s(t)$ is given by the product of energy-temperature ratios ($E/(k_B T)$, $\ln \epsilon$) and the temperature evolution expressed as $\frac{d \ln T}{d \ln t}$. The conditions in which the temperature variation significantly affects the roughness are similar to our model: $|s(t)| \sim 1$. Thus, in room temperature conditions and with activation energy sets similar to the one studied here, the same features of the roughness evolution are expected.

These results suggest the investigation of temperature variation during the deposition of a film in all cases where surface dynamics is dominated by adatom diffusion and where features such as AS, large growth exponents (possibly in a small time range), or nonmonotonic variation of roughness are observed.

7. Conclusion

We studied a thin film growth model in which the surface diffusion coefficients of adsorbed species are related to the substrate/film temperature in conditions where that temperature increases or decreases during the deposition. The model assumes that only adatoms in terraces can move, so that a single parameter determines scaling properties.

Cases of temperature varying linearly in time and of an exponential convergence to a final temperature were separately analyzed, the later representing systems exchanging heat by conduction with a thermal reservoir. In all cases, 10^4 atomic layers were grown with temperatures in the range of room temperature or below and variations during the growth up to 30K, which are feasible conditions with many experimental techniques.

If the temperature decreases during the growth, the global roughness slowly increases at short times but eventually turns to be a rapidly increasing function of time. In several cases, effective growth exponents $\beta_{eff} > 1/2$ are obtained in the thickness range $10^3 ML < t < 10^4 ML$. This shows that the simple physical

mechanism of reducing the temperature during the growth may lead to a nontrivial roughness evolution, which is usually related to more complicated mechanisms, such as step energy barriers or shadowing. The local roughness shows evidence of anomalous scaling in the thickness range analyzed. In the cases of linear temperature decrease, the local roughness in a small box size may increase in time even faster than a power law. In the cases of exponential convergence to a final temperature, several values of the anomaly exponent may be obtained.

If the temperature increases during the growth, a non-monotonic evolution of the global roughness may be observed. In cases of linear temperature increase, a maximum of roughness is usually observed, being more pronounced for lower temperature ranges. In the case of exponentially converging temperature, a maximum and a minimum may be observed (eventually turning into a plateau in the $\log_{10}(W) \times \log_{10}(t)$ plot). These features are interpreted as a consequence of competition of kinetic roughening, which leads to roughness increase, and the smoothing effect of increasing diffusion coefficients.

Stochastic growth equation approaches [15] and lattice models [18] have already considered the effect of time-varying couplings in interface growth, with emphasis on anomalous scaling properties. The main advance of the present work is to show that a series of nontrivial features of surface roughness scaling (including anomalous scaling) appear in realistic conditions of film growth. Moreover, our results shown very good agreement with theoretical predictions in all the cases studied. In the growth regime, that approach may help to predict conditions for observing the same phenomena observed here, such as AS and rapid roughness increase (large β_{eff}) for decreasing temperature and roughness oscillations for increasing temperature.

Finally, we note that results equivalent to the ones obtained with varying temperature (i. e. varying D) may be obtained with variable flux F , since the main parameter of our model is the ratio R . This is particularly interesting for possible experimental tests, since controlling the deposition flux is usually easier than the temperature.

Acknowledgements

The authors thank Prof. F. de B. Mota for fruitful discussions and valuable suggestions to optimize the computational work. The authors also acknowledge support from CNPq and FAPERJ (Brazilian agencies).

References

- [1] M. Ohring, *Materials Science of Thin Films - Deposition and Structure*, 2nd. ed., Academic Press, 2001.
- [2] A. Pimpinelli and J. Villain, *Physics of Crystal Growth* (Cambridge University Press, Cambridge, England, 1998).
- [3] A. L. Barabási and H. E. Stanley, *Fractal concepts in surface growth*, Cambridge University Press, 1995.
- [4] J. W. Evans, P. A. Thiel, and M. C. Bartelt, Surf. Sci. Rep. **61**, 1 (2006).
- [5] F. Family and T. Vicsek, J. Phys. A **18** L75 (1985).
- [6] S. Huo and W. Schwarzacher, Phys. Rev. Lett. **86**, 256 (2001).
- [7] W. Schwarzacher, J. Phys. Condensed Matter **16**, R859 (2004).
- [8] J. M. López, Phys. Rev. Lett. **83**, 4594 (1999).
- [9] J. M. López and M. A. Rodríguez, Phys. Rev. E **54**, R2189 (1996).
- [10] M. A. Auger, L. Vázquez, R. Cuerno, M. Castro, M. Jergel, and O. Sánchez, Phys. Rev. B **73**, 045436 (2006).

- [11] M. F. Alamini, R. C. da Silva, V. C. Zoldan, E. A. Isoppo, U. P. Rodrigues Filho, F. D. A. Aarão Reis, A. N. Klein, and A. A. Pasa, *Electrochem. Comm.* **13**, 1455 (2011).
- [12] M. Alava, M. Dubé, and M. Rost, *Adv. Phys.* **53**, 83 (2004).
- [13] Y.-L. Chou, M. Pleimling, and R. K. P. Zia, *Phys. Rev. E* **80**, 061602 (2009).
- [14] S.F. Edwards and D.R. Wilkinson, *Proc. R. Soc. London* **381**, 17 (1982).
- [15] M. Pradas, J. M. López, and A. Hernández-Machado, *Phys. Rev. E* **76**, 010102(R) (2007).
- [16] M. Dubé, M. Rost, K. R. Elder, M. Alava, S. Majaniemi, and T. Ala-Nissila, *Phys. Rev. Lett.* **83**, 1628 (1999).
- [17] M. Pradas and A. Hernández-Machado, *Phys. Rev. E* **74**, 041608 (2006).
- [18] F. D. A. Aarão Reis, *Phys. Rev. E* **84**, 031604 (2011).
- [19] F. D. A. Aarão Reis, *Phys. Rev. E* **81**, 041605 (2010).
- [20] S. Das Sarma and P. Tamborenea, *Phys. Rev. Lett.* **66** (1991) 325.
- [21] R. L. Schwoebel, *J. Appl. Phys.* **44**, 614 (1969).
- [22] J. W. Evans, D. K. Flynn-Sanders, and P. A. Thiel, *Surf. Sci.* **298**, 378 (1993).
- [23] A. Chame and F. D. A. Aarão Reis, *Surf. Sci.* **553**, 145 (2004).
- [24] C. M. Horowitz and E. V. Albano, *Phys. Rev. E* **73**, 031111 (2006).
- [25] F. D. A. Aarão Reis, *Phys. Rev. E* **73**, 021605 (2006).
- [26] M. M. Schwickert, K. A. Hannibal, M. F. Toney, M. Best, L. Folks, J.-U. Thiele, A. J. Kellock, and D. Weller, *J. Appl. Phys.* **87**, 6956 (2000).
- [27] J. Candia and E. V. Albano, *J. Stat. Mech.* P08006 (2012).
- [28] S. Das Sarma, C. J. Lanczycki, R. Kotlyar, and S. V. Ghaisas, *Phys. Rev. E* **53**, 359 (1996).
- [29] M. Kotrla and P. Smilauer, *Phys. Rev. B* **53**, 13777 (1996).
- [30] M. R. Wilby, D. D. Vvedensky, and A. Zangwill, *Phys. Rev. B* **46**, 12896(R) (1992).
- [31] Z.-W. Lai and S. Das Sarma, *Phys. Rev. Lett.* **66**, 2348 (1991).
- [32] J. Villain, *J. Phys. I* **1**, 19 (1991).
- [33] C. A. Haselwandter and D. D. Vvedensky, *Europhys. Lett.* **77**, 38004 (2007).
- [34] C. A. Haselwandter and D. D. Vvedensky, *Phys. Rev. E* **77**, 061129 (2008).
- [35] H. K. Janssen, *Phys. Rev. Lett.* **78**, 1082 (1997).
- [36] F. D. A. A. Reis, *Phys. Rev. E* **70**, 031607 (2004).
- [37] F. F. Leal, T. J. Oliveira, and S. C. Ferreira, *J. Stat. Mech.* P09018 (2011).
- [38] H. Xia, G. Tang, Z. Xun, and D. Hao, *Surf. Sci.* **607**, 138 (2013).
- [39] K. J. Caspersen, A. R. Layson, C. R. Stoldt, V. Fournee, P. A. Thiel, and J. W. Evans, *Phys. Rev. B* **65**, 193407 (2002).
- [40] A. Yanguas-Gil, J. Cotrino, A. Barranco, and A. R. Gonzalez-Eliphe, *Phys. Rev. Lett.* **96** 236101 (2006).
- [41] S. W. Son, M. Ha, and H. Jeong, *J. Stat. Mech.* P02031 (2009).
- [42] T. J. Oliveira and F. D. A. Aarão Reis, *J. Appl. Phys.* **101**, 063507 (2007).
- [43] M. Kardar, G. Parisi and Y.-C. Zhang, *Phys. Rev. Lett.* **56** 889 (1986).
- [44] T. Nattermann and L.-H. Tang, *Phys. Rev. A* **45**, 7156 (1992).
- [45] M. Santos, W. Cavalcanti, A. A. Pasa, and W. Figueiredo, *Physica A* **308**, 313 (2002).
- [46] S. Pal and D. P. Landau, *Computational Materials Science* **6**, 176 (1996).
- [47] D. P. Landau and S. Pal, *Thin Solid Films* **272**, 1841 (1996).
- [48] S. Clarke and D. D. Vvedensky, *J. Appl. Phys.* **63**, 2272 (1988).
- [49] M. C. Bartelt, L. S. Perkins, and J. W. Evans, *Surf. Sci. Lett.* **344**, L1193 (1995).
- [50] T. J. Oliveira and F. D. A. Aarão Reis, *Phys. Rev. B*, **87**, 235430 (2013).